CACOXENITE IN MIOCENE SEDIMENTS OF THE MARYLAND COASTAL PLAIN

Paul P. Hearn, Jr., Lucy McCartan, David R. Soller,
M. Dennis Krohn, and Virginia M. Gonzalez

U.S. Geological Survey, Reston, Virginia 22092

Abstract—Cacoxenite having the composition $(Al_{4.0}Fe_{22.5}O_{7.1}(OH)_{14.3}(PO_4)_{17}(H_2O)_{23.7}) \cdot 50.3H_2O$ was identified in a bed of mature quartz sand in the Miocene Calvert Formation near Popes Creek, Maryland. This is the first reported occurrence of this mineral in Atlantic Coastal Plain sediments north of Florida. The cacoxenite occurs as silt-size to sand-size grains, both as irregularly shaped aggregates and as radiating arrays of delicate acicular crystals. The presence of discrete cores and overgrowths in some grains indicates at least two generations of crystal growth. Electron microprobe analyses reveal excess Si and Al (relative to the ideal composition), which is believed to reflect ultra-fine clay particles within the cacoxenite grains. Admixed clays probably served as a substrate for the formation of ferric oxyhydroxides, which were subsequently converted to cacoxenite through the addition of dissolved phosphorus.

Key Words—Cacoxenite, Genesis, Iron oxyhydroxides, Overgrowths, Phosphorus.

INTRODUCTION

Previous workers have described samples of pure cacoxenite (Moore and Shen, 1983) and discussed thermochemical constraints on their formation (Nriagu and Moore, 1984; Nriagu and Dell, 1974). In this paper we present the results of electron microprobe, X-ray powder diffraction, and infrared analyses of an intimate mixture of cacoxenite and clay in unconsolidated Miocene sediments near Popes Creek, Maryland. These findings are significant because they represent the first report of cacoxenite in the Atlantic Coastal Plain outside of the Florida phosphate district and the bog iron ore area of New Jersey, and because they suggest that clay minerals may play an important role as a substrate for cacoxenite formation.

GEOLOGIC SETTING

The U.S. Geological Survey has investigated weathering processes in Coastal Plain units for two decades (see, e.g., Owens *et al.,* 1983; McCartan *et al.,* 1984). The Popes Creek locality is one of hundreds of vertical sections which have been studied in considerable detail; it was during these routine investigations that cacoxenite was discovered. The cacoxenite occurs in a 20-cm-thick bed of unconsolidated yellow-orange sand 12 m below the top of a cliff along the Potomac River, about 0.5 km south of Popes Creek, Maryland. The sand bed is immediately below the contact between the marine Miocene Calvert Formation and overlying Pliocene-Pleistocene estuarine deposits, and has been traced laterally for about 15 m. The yellow-orange sand is within the weathered part of the Calvert, which is several meters thick; unweathered material lower in the cliff is richer in clay and is greenish black. The basal beds of the overlying unit consist primarily of poorly sorted pebbly sand with a mud matrix and lenses of fine sand. In addition to cacoxenite, the weathered Calvert consists primarily of rounded grains of quartz, minor amounts of kaolinite, illite, expandable clay minerals, goethite, and a suite of heavy minerals dominated by ilmenite. The relative concentration of cacoxenite (estimated from total phosphorus analyses) varies from 1 to 2 wt. % at the top of the bed to as much as 30 wt. % at the base. Cacoxenite does not appear to be widespread within the Calvert Formation; careful examination of several other outcrops revealed no additional occurrences.

EXPERIMENTAL

Cacoxenite and associated minerals were analyzed by means of X-ray powder diffractometry (XRD), a scanning electron microscope equipped with an energy-dispersive X-ray analyzer (SEM/EDX), an electron microprobe, optical microscopy, and infrared spectroscopy (IR). Samples analyzed by XRD and IR were purified from the water-sieved, fine-sand fraction of bulk samples by repeated magnetic separation and cleaning in an ultrasonic bath. Samples examined by SEM/EDX, microprobe, and optical microscopy were less pure in a bulk sense, but only individual massive grains and aggregates of cacoxenite were analyzed. With the latter techniques, we accepted the impurities in order to avoid damage to crystallites caused by the cleaning process. Oriented mounts were prepared for XRD by sedimenting aqueous suspensions of <2-μm material onto glass slides. A sodium citrate-bicarbonate-dithionite (CBD) extraction technique (Jackson, 1975) was used to remove cacoxenite from sample splits for more effective characterization of admixed clay minerals. Some of the XRD preparations were
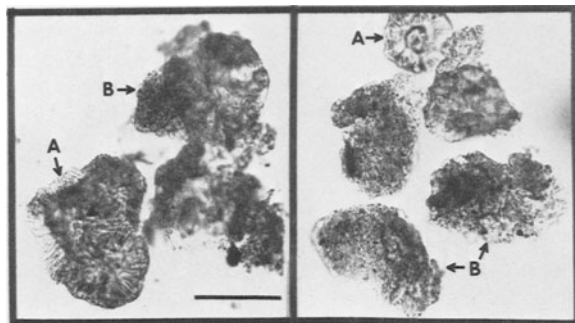
419

Figure 1. Photomicrographs of cacoxenite grains, showing radiating acicular habit (A) and irregularly shaped aggregates (B). Bar is 50 μm.

Table 1. X-ray powder diffraction data for Popes Creek, Maryland, cacoxenite.

hkl	JCPDS 14-331 d (Å)	Popes Creek cacoxenite d (Å)
100	23.1	23.9[1]
200	11.9	11.9
101	9.7	9.8
210	9.1	9.0
300,201	8.0	7.9
321,112	4.90	4.89
601	3.73	3.72
710,303	3.18	3.17

[1] In separate diffractometer scans, the d(100) spacing appeared as a broad band of reflections from 23.7 to 25.2 Å at room temperature and from 23.5 to 24.8 Å on heating for 1 hr at 50°C.

glycolated overnight, and others were heated between 50° and 550°C for 1 hr. The treated and untreated samples were analyzed on a Diano X-ray diffractometer using CuKα radiation. Clay mineral proportions were determined semiquantitatively by a method modified by one of the authors (Soller) from the technique of Johns *et al.* (1954) and H. D. Glass (Illinois State Geological Survey, Champaign, Illinois, personal communication, 1986). The relative abundances of the various clay minerals admixed with the cacoxenite were estimated from the XRD trace of a glycolated sample supplemented by traces of heated specimens (for analysis of kaolinite).

Polished grain mounts of magnetically separated cacoxenite were analyzed on an ARL SEMQ electron microprobe at an operating voltage of 15 kV and a beam current of 50 nA, using a combination of synthetic and natural standards. Polished grain mounts were also examined with an ETEC Autoscan scanning electron microscope (SEM) equipped with a backscattered-electron detector and an EDAX 9100 X-ray analyzer (EDX).

Visible and near-infrared (near-IR) spectra were measured on a Beckman model 5240 UV spectrophotometer before and after heating. A sample of purified cacoxenite from the Calvert Formation was handpicked for IR analysis to avoid surface coatings on the grains, because of the sensitivity of near-IR techniques to coatings.

RESULTS AND DISCUSSION

Composition and habit of cacoxenite

The cacoxenite was first identified by XRD on the basis of characteristic d-values (Table 1). It occurs both as irregularly shaped yellow-brown aggregates and as radiating arrays of acicular crystals (Figure 1). Indices of refraction are between 1.647 and 1.666; crystals are uniaxial positive and length slow, and the c-axis is parallel to the fast ray.

The composition of cacoxenite was computed from the average of three microprobe point analyses that showed only P, Fe, and Al (Table 2). A structural formula was then computed from these results by normalizing to the tetrahedral ion (P) and partitioning structurally bound and adsorbed water according to the idealized formula from the X-ray structural study of Moore and Shen (1983). Total water was assumed to be equivalent to the difference between the total of the electron microprobe analysis and 100%. The formula computed from probe analyses is in good agreement with the idealized formula and indicates the maximum allowable substitution of Al for Fe in octahedral sites (Table 2). Some grains contain as much as 3.5 wt. % Si, which is probably present as finely disseminated aluminosilicate material, as evidenced by the correlation of Si with Al (r = .80 for 20 analyses) and the lack of any corresponding variation in the Fe/P ratio. A few quartz grains were also found attached to cacoxenite.

Backscattered-electron SEM micrographs show that a few of the cacoxenite grains contain cores, which are significantly darker than the surrounding overgrowths, indicating that the average atomic weight of the cores is lower than that of the overgrowths (Figure 2). EDX analyses normalized on a water-free basis show no significant difference in the relative proportions of Fe, P, and Al in cores and overgrowths (Figure 3). These results suggest that the discrepancy in average atomic weight is due to an excess of water in the cores relative to the overgrowths. All other iron-aluminum phos-

Table 2. Chemical composition (oxide weight percent) and structural formula for Popes Creek cacoxenite.

Al_2O_3	Fe_2O_3	P_2O_5	H_2O (by difference)
4.4	38.3	25.7	31.6

Idealized formula (Moore and Shen, 1983):
$(Al(Al,Fe)_3Fe_{21}O_6(OH)_{12}(PO_4)_{17}(H_2O)_{24})\cdot 51\ H_2O$
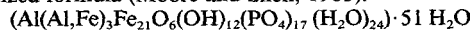
Formula computed from the average of three electron probe analyses:
$(Al_{4.0}Fe_{22.5}O_{7.1}(OH)_{14.3}(PO_4)_{17}(H_2O)_{23.7})\cdot 50.3\ H_2O$

Figure 2.   Backscattered-electron micrograph of cacoxenite aggregates showing distinct cores and overgrowths. Relative backscattered intensities indicate that cores have lower average atomic weight than overgrowths. Darkened areas in central portion of cores are topographic artifacts caused by the plucking of material during polishing of the sample surface. Bar is 10 μm.
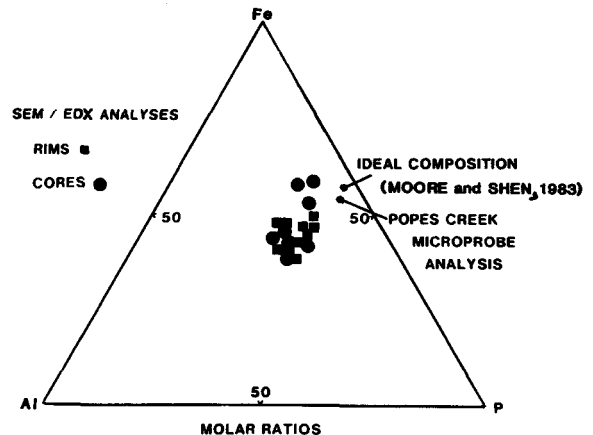

Figure 3.   Relative molar proportions of Fe, Al, and P in cores and overgrowths of two-generation grains of cacoxenite (analyses by energy dispersive X-ray spectroscopy). Microprobe value is average of three analyses.

phate minerals are less hydrated than cacoxenite; this fact, plus the similar proportions of Fe, Al, and P, suggests that the cores and overgrowths represent two different hydration states of cacoxenite. The discrepancy in the 100 spacing between the Popes Creek cacoxenite and the JCPDS standard reference sample suggests that the Popes Creek sample may be slightly more hydrated (Table 1). Furthermore, heating a concentrate of the Popes Creek cacoxenite at 50°C for 1 hr reduced the 100 spacing by 0.2–0.6 Å (see footnote to Table 1). These findings are consistent with the results of structural studies which suggest that the cacoxenite structure can accommodate more water than that indicated by the idealized formula (P. B. Moore, University of Chicago, Chicago, Illinois, personal communication, 1986).

Infrared spectroscopy

Visible and near-infrared spectra were obtained to determine the electronic configuration of iron in the cacoxenite structure and, more importantly, to determine whether aluminum-hydroxyl (Al–OH) bonds are an integral part of the structure. The spectrum of the cacoxenite-clay mixture (Figure 4b) shows the characteristic absorption features of Fe and Al–OH. A relatively broad absorption feature at 0.9 μm, a sharp fall-off between 0.7 and 0.5 μm, and an inflection at 0.5 μm are attributable to crystal field transitions of ferric iron (Sherman *et al.*, 1982). The shape of the fall-off in the visible range and the inflection at 0.5 μm are particularly characteristic. Of several iron oxide polymorphs, the spectrum of cacoxenite most closely resembles that of ferrihydrite, a poorly crystalline to noncrystalline iron hydroxide (Sherman *et al.*, 1982).

The remaining bands in the cacoxenite-clay spec-

trum (Figure 4b) are related to different forms of hydroxyl. The band at 1.4 μm is attributable to OH-stretching vibrations, and the band at 1.9 μm is attributable to bending modes of molecular water (Hunt and Salisbury, 1970). The broadening of the 1.4- and 1.92-μm bands toward longer wavelengths indicates that the hydroxyl sites are relatively disordered and that hy-
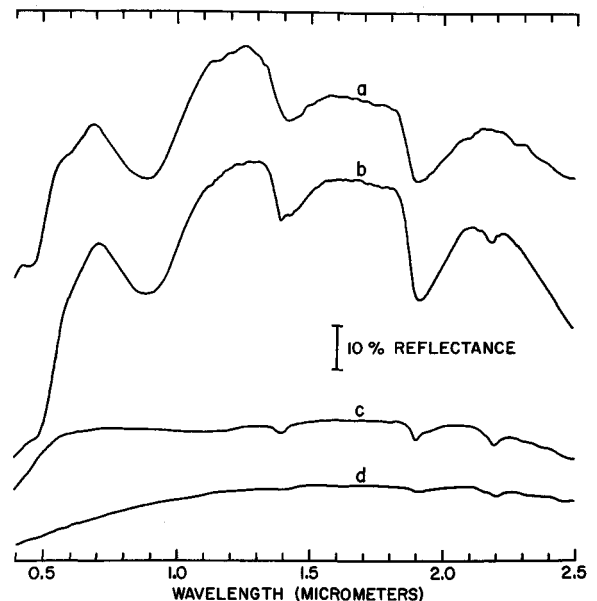

Figure 4.   Visible/near-infrared spectra: (a) Reference spectrum of pure cacoxenite (secondary alteration of bog iron ore near Lancaster, Pennsylvania; Smithsonian Institution specimen #C4358-1); (b) spectrum of cacoxenite-clay separate from the Popes Creek section; (c) Popes Creek sample following removal of cacoxenite by CBD extraction; (d) Popes Creek sample following citrate-bicarbonate-dithionite extraction and heating at 350°C. All reflectance values measured relative to halon.

drogen bonding might be present. The band at 2.2 μm is directly attributable to Al–OH bonds; the remaining question is whether the Al–OH feature is related to the cacoxenite structure itself or is attributable solely to admixed clay minerals. Two lines of evidence suggest the latter. A spectrum of the cacoxenite-free residue remaining after the CBD extraction of the cacoxenite-clay mixture is shown in Figure 4c. The Al–OH feature at 2.2 μm is still present and has about the same band depth as that recorded for the mixture of clay and cacoxenite. Also, a spectrum of a reference sample of pure cacoxenite from Pennsylvania (Figure 4a) shows no absorption feature for Al–OH.

The O–H and H–O–H bands at 1.4 and 1.9 μm are present in the spectra of both the cacoxenite-clay mixture and the CBD-extracted sample, but the band depths are much greater in the sample containing the cacoxenite. This indicates that most of the disordered water is associated with the cacoxenite rather than with admixed clay minerals. The presence of the 1.9- and 2.2-μm bands together in the CBD-extracted sample indicates bonded water in clay minerals. Removal of most of the water in the clay upon partial heating of the sample to 350°C is indicated by reduction of the 1.9-μm band (Figure 4d). Traces of the Al–OH bond are still present, as indicated by the 2.2-μm band.

Clay minerals admixed with cacoxenite

Clay minerals, undetected prior to the extraction procedure, were identified in the residue of the CBD-treated cacoxenite sample. Admixed cacoxenite may have limited the degree of preferred orientation and the intensity of the basal reflections of the clay minerals. Traces of CBD-extracted and glycolated clay samples (Figure 5) show peaks of disordered kaolinite (broad, low-angle asymmetric 7-Å peak), well-ordered illite (sharp 10-Å peak that did not shift on glycolation), and a randomly interstratified expandable material, probably a smectite-dominated illite/smectite (recorded as a broad peak centered near 15 Å in traces of untreated samples and as a broad diffraction band at about 17–22 Å in traces of glycolated samples). Detrital quartz was also identified but was disregarded because it was assumed merely to be part of the inert grain framework. The sample was then X-rayed after heating for 1 hr at 150°, 350°, 450°, 500°, and 550°C (Figure 5). Predictably, the expandable material dehydrated irreversibly to a 10-Å spacing on heating to 150°C. The kaolinite, which shows a broad basal reflection at 7 Å indicative of disorder, was not affected by heating to this temperature. The disordered kaolinite was also unaffected by heating to 350°C. On heating the sample to 450°C, only a small and symmetrical 7-Å peak remained, indicating the destruction of disordered kaolinite and the persistence of a minor amount of ordered kaolinite. The disordered kaolinite is apparently
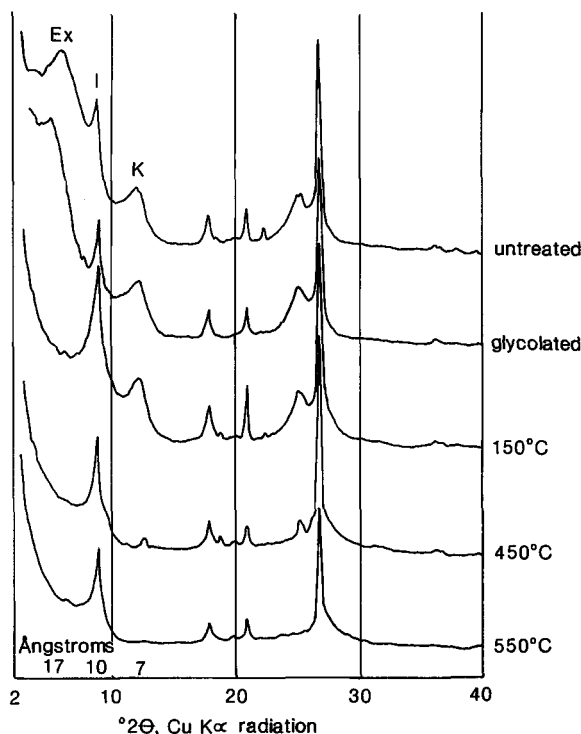

Figure 5. X-ray powder diffractograms showing the effects of ethylene glycol and heat treatment of clay minerals in the <2-μm size fraction of material from the cacoxenite-rich zone. Cacoxenite was removed by sodium citrate-bicarbonate-dithionite extraction. Dehydration and collapse of expandable material (Ex) occurs on heating to 150°C; basal reflection of expandable material collapses to 10 Å, coinciding with the basal illite peak (I). Most kaolinite (K) is destroyed on heating to 450°C.

not hydrated, because its structure was unaffected by heat treatment until it underwent complete destruction at 450°C. The ordered kaolinite broke down, predictably, at 550°C. Based on peak intensities following the 350°C and 450°C treatments, the relative proportions of disordered and ordered kaolinite were estimated to be 90% and 10%, respectively. The clay suite contains about 44% disorderd kaolinite, 31% illite, 21% expandable material (probably a randomly interstratified illite/smectite dominated by smectite), and 4% ordered kaolinite.

Ultra-fine grained clay minerals may also be present within individual cacoxenite grains. SEM/EDX analyses showed that most cacoxenite grains are enriched in Si and Al relative to both the ideal formula and the formula computed from electron probe analyses. The fact that SEM analyses revealed no discrete clay particles within the cacoxenite grains suggests the presence of aluminosilicate crystallites considerably smaller than 1 μm. Such material may be physically incorporated precursor clays or secondary clay minerals that coprecipitated with the cacoxenite.
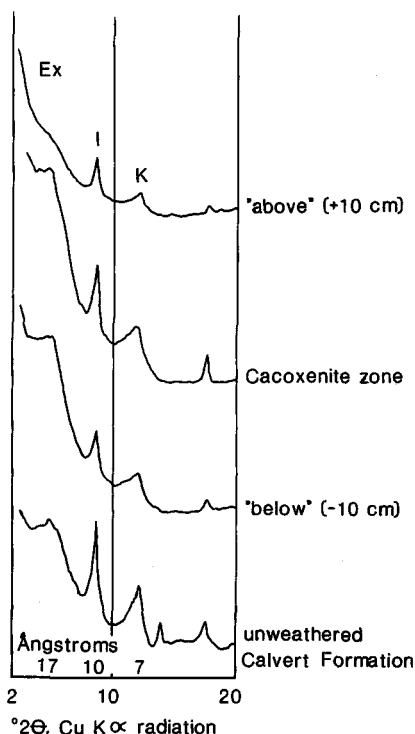
Figure 6. Distribution of clay minerals in part of the Calvert Formation at Popes Creek, Maryland. All samples were treated with ethylene glycol and citrate-bicarbonate-dithionite-extracted to remove cacoxenite and iron oxides. Symbols same as for Figure 5.

Table 3. Semi-quantitative clay mineral analyses based on X-ray powder diffractograms.[1]

Sample	Expand-able material (%)	Illite (%)	Kaolinite (%)
Above cacoxenite zone[2]	14	46	40
Cacoxenite zone	21	31	48
Below cacoxenite zone[3]	31	30	39
Unweathered Calvert Formation[4]	22	49	29

[1] Because this semi-quantitative analysis cannot measure clay minerals that have weathered and become amorphous to X-rays (probably of the expandable group), the relative percentage of illite and kaolinite in the "above" sample may be high and misleading, and the absolute quantity of either of these minerals may be somewhat lower.
[2] Sampled near top of Calvert Formation, about 10 cm above cacoxenite zone.
[3] Sampled about 10 cm below cacoxenite zone in Calvert Formation.
[4] Sampled about 2 m below cacoxenite zone in less weathered part of Calvert Formation.

Clay mineral trends in the upper part of the Calvert Formation

The crystallinities of kaolinite and illite in the three samples in and near the cacoxenite zone were similar; however, the expandable material in the upper sample was noticeably less ordered and less homogenous than that in the lower two samples (Figure 6 and Table 3). These differences are probably due to more intense weathering in the uppermost part of the Calvert Formation. Although the degree of chemical weathering was probably greater in the cacoxenite zone than in the underlying sample, the crystallinity of the clay minerals is essentially the same in these two samples. Relative to the lower sample, however, the cacoxenite sample is enriched in kaolinite at the expense of the expandable material. The proportion of kaolinite in the upper sample is also greater.

Paragenesis

Cacoxenite forms most commonly by the alteration of a precursor phase (Nriagu and Moore, 1984). Although direct precipitation from pore waters is thermodynamically possible, evidence for such an origin in nature is lacking. The alteration of bone-derived hydroxyl-phosphate or igneous apatite to cacoxenite is not likely (Nriagu and Moore, 1984); however, these

sources may play a role through intermediate phases. Vivianite is probably the most stable ferrous phosphate found in natural environments (Nriagu, 1972) and has been identified both in Maryland Coastal Plain sediments (L. McCartan, unpublished data) and in sediments of the Chesapeake Bay (Bricker and Troup, 1975). Thermochemical studies indicate, however, that cacoxenite is not a primary product of the oxidation of vivianite, but is more likely to form by the interaction of phosphate ions with Fe-Mn oxides and hydroxides (Nriagu and Dell, 1974). Ferric oxyhydroxides occur commonly in freshwater sediments as colloidal gels or coatings on the surfaces of clay minerals (Carroll, 1958). They have been reported in surface sediments of the Potomac River in concentrations as high as 2 wt. % as Fe (Piercey, 1981). The data of Hearn et al. (1983) on Potomac River surface sediments suggest that noncrystalline ferric hydroxy-phosphates form preferentially to vivianite in the presence of ferric oxyhydroxides. Although no cacoxenite was identified in the sediments, pore waters were shown to be supersaturated with respect to this phase throughout most of the tidal freshwater portion of the estuary.

The most recent generation of cacoxenite almost certainly formed in situ, as the delicate arrays of acicular crystals show no evidence of mechanical abrasion during transport (Figure 2). In contrast, many of the earlier generation grains have irregular or angular cross sections. Although these irregularities may reflect partial dissolution in place due to changing physicochemical conditions, this generation of cacoxenite may also have formed elsewhere and have been abraded during transport.

Ferric oxyhydroxides may have formed in Calvert sediments during early diagenesis at the original sediment-water interface or during later diagenesis by per-

colating ground water following uplift. The lack of physical or chemical abrasion suggests that the second generation of cacoxenite precipitated by the sorption of dissolved phosphorus from ground water onto ferric oxyhydroxides. The early-stage cacoxenite may have formed in the same manner; however, the apparent thermochemical stability of cacoxenite in present-day Potomac sediments and the angular shape of the early-stage aggregates suggest that this generation of cacoxenite may also have formed in a riverine environment.

A more detailed discussion of paragenetic models is not warranted by the information available at the present time; however, the occurrence of cacoxenite in the Calvert Formation can probably be explained by local chemical inhomogeneities which served to mobilize and transport dissolved phosphorus. Numerous scenarios are possible, including (but not limited to) the release of phosphorus from coexisting organic matter and the mobilization and concentration of dissolved phosphorus by local inhomogeneities in pore-water/ground-water eH or pH. Cacoxenite most likely formed by the sorption of dissolved phosphorus onto ferric oxyhydroxides that coated preexisting clay minerals. The clays acted as a substrate for the formation of ferric oxyhydroxides and provided a source of Al for the cacoxenite.

ACKNOWLEDGMENTS

REFERENCES

Bricker, O. P. and Troup, B. N. (1975) Sediment-water exchange in the Chesapeake Bay: in *Estuarine Research* **1,** 3–27.

Carroll, D. (1958) Role of clay minerals in the transportation of iron: *Geochim. Cosmochim. Acta* **14,** 1–27.

Hearn, P. P., Parkhurst, D. L., and Callender, E. (1983) Authigenic vivianite in Potomac River sediments: control by ferric oxyhydroxides: *J. Sed. Petrol.* **53,** 165–177.

Hunt, G. R. and Salisbury, J. W. (1970) Visible and near-infrared spectra of minerals and rocks. I. Silicate minerals: *Modern Geology* **1,** 283–300.

Jackson, M. L. (1975) *Soil Chemical Analysis—Advanced Course:* 2nd ed., 10th printing, published by author, Dept. Soil Science, University of Wisconsin, Madison, Wisconsin, 895 pp.

Johns, W. D., Grim, R. E., and Bradley, W. F. (1954) Quantitative estimations of clay minerals: *J. Sed. Petrol.* **24,** 242–251.

McCartan, L., Lemon, E. M., Jr., and Weems, R. E. (1984) Geology of the area between Charleston and Orangeburg, South Carolina: *U.S. Geol. Surv. Map* **I-1472.**

Moore, P. B. and Shen, J. (1983) An X-ray structural study of cacoxenite, a mineral phosphate: *Nature* **306,** 356–358.

Nriagu, J. O. (1972) Stability of vivianite and ion-pair formation in the system $Fe_3(PO_4)-2H_3PO_4-H_2O$: *Geochim. Cosmochim. Acta* **36,** 459–470.

Nriagu, J. O. and Dell, C. I. (1974) Diagenetic formation of iron phosphates in recent lake sediments: *Amer. Mineral.* **59,** 934–946.

Nriagu, J. O. and Moore, P. B. (1984) *Phosphate Minerals:* Springer-Verlag, New York, 442 pp.

Owens, J. P., Hess, M. M., Denny, C. S., and Dwornik, E. J. (1983) Postdepositional alteration of surface and near-surface minerals in selected Coastal Plain Formations of the middle Atlantic States: *U.S. Geol. Surv. Prof. Pap.* **1067-F,** 45 pp.

Piercey, E. J. (1981) Phosphate sorption on clay-rich channel sediments of the tidal Potomac River and estuary: *Estuaries* **4,** 251 (abstract).

Sherman, D. M., Burns, R. C., and Burns, V. M. (1982) Spectral characteristics of the iron oxides with application to Martian bright region mineralogy, *J. Geophys. Res.* **87,** 10169–10180.